Neurobiology of Aging 74 (2019) 191–201

Contents lists available at ScienceDirect

Neurobiology of Aging

journal homepage: www.elsevier.com/locate/neuaging

Amyloid beta–positive subjects exhibit longitudinal network-specific reductions in spontaneous brain activity

Brian B. Avants [a,*], R. Matthew Hutchison [b], Alvydas Mikulskis [a], Cristian Salinas-Valenzuela [b], Richard Hargreaves [c], John Beaver [b], Ping Chiao [b], for the Alzheimer's Disease Neuroimaging Initiative [1]

[a] Biogen employee while completing work, 225 Binney Street, Cambridge, Massachusetts, 02142, USA
[b] Biogen, 225 Binney Street, Cambridge, Massachusetts, 02142, USA
[c] Celgene, 86 Morris Avenue, Summit, New Jersey, 07901, USA

ARTICLE INFO

Article history:
Received 1 February 2018
Received in revised form 6 September 2018
Accepted 2 October 2018
Available online 11 October 2018

Keywords:
Alzheimer's disease
Amyloid beta
Fluorodeoxyglucose positron emission tomography
Reference region spontaneous brain activity
Resting-state functional magnetic resonance imaging

ABSTRACT

Amyloid beta (Aβ) deposition and cognitive decline are key features of Alzheimer's disease. The relationship between Aβ status and changes in neuronal function over time, however, remains unclear. We evaluated the effect of baseline Aβ status on reference region spontaneous brain activity (SBA-rr) using resting-state functional magnetic resonance imaging and fluorodeoxyglucose positron emission tomography in patients with mild cognitive impairment. Patients (N = 62, [43 Aβ-positive]) from the Alzheimer's Disease Neuroimaging Initiative were divided into Aβ-positive and Aβ-negative groups via prespecified cerebrospinal fluid Aβ42 or 18F-florbetapir positron emission tomography standardized uptake value ratio cutoffs measured at baseline. We analyzed interaction of biomarker-confirmed Aβ status with SBA-rr change over a 2-year period using mixed-effects modeling. SBA-rr differences between Aβ-positive and Aβ-negative subjects increased significantly over time within subsystems of the default and visual networks. Changes exhibit an interaction with memory performance over time but were independent of glucose metabolism. Results reinforce the value of resting-state functional magnetic resonance imaging in evaluating Alzheimer"s disease progression and suggest spontaneous neuronal activity changes are concomitant with cognitive decline.

1. Introduction

Alzheimer's disease (AD) pathophysiology can precede cognitive symptoms by decades and is characterized by alterations in amyloid beta (Aβ) production and clearance, formation of β-amyloid plaques, and accumulation of neurofibrillary tangles (Braak et al., 1999; Dubois et al., 2016; Hardy and Selkoe, 2002a; Jack et al., 2009). Pathophysiological processes characterize disease stage and AD subtype (Ennis et al., 2017; Hall et al., 2013; Soldan et al., 2013) such that the progressive evolution of AD can be modeled using fluid and imaging biomarkers that correlate with functional decline (Jack et al., 2010; Jack and Holtzman, 2013). Recent studies suggest that optimal prognostic and diagnostic biomarkers of AD (Cavedo et al., 2014; Kandel et al., 2015a, 2016; Toledo et al., 2015) may differ from optimal biomarkers for tracking AD progression (Egli et al., 2015; Mattsson et al., 2015; Mazzeo et al., 2016) and from biomarkers that predict timing of cognitive decline (Berenguer et al., 2014; Choo et al., 2013; Degerman Gunnarsson et al., 2016; Portelius et al., 2015; Toledo et al., 2014).

Measures of brain function have emerged as potential candidates for evaluating AD progression (Iturria-Medina et al., 2016). Recent studies have highlighted the importance and early emergence of cerebral neurovascular dysfunction and sequelae in AD (Iturria-Medina et al., 2016; Taylor et al., 2017) that, along with abnormal protein deposition, may represent early manifestations of AD pathophysiology (Edmonds et al., 2015; Hardy and Selkoe, 2002b; Iturria-Medina et al., 2016). Resting-state functional magnetic resonance imaging (rs-fMRI) can be used to investigate the complex spatiotemporal mechanisms of brain function through the characterization of spontaneous blood oxygen level–dependent (BOLD) fluctuations (Fox and Raichle, 2007; Shmuel and Leopold,

* Corresponding author at: 225 Binney Street, Cambridge, MA, 02142, USA. Tel.: 914 454 5757; fax: 855 547 5259.
E-mail address: stnava@gmail.com (B.B. Avants).

[1] Data used in preparation of this article were obtained from the Alzheimer's Disease Neuroimaging Initiative (ADNI) database (adni.loni.usc.edu). As such, the investigators within the ADNI contributed to the design and implementation of ADNI and/or provided data but did not participate in analysis or writing of this report. A complete listing of ADNI investigators can be found at: http://adni.loni.usc.edu/wp-content/uploads/how_to_apply/ADNI_Acknowledgement_List.pdf.

0197-4580/$ – see front matter © 2018 Published by Elsevier Inc.
https://doi.org/10.1016/j.neurobiolaging.2018.10.002

2008). BOLD fluctuations are the result of neuronal firing activity (Hutchison et al., 2015; Scholvinck et al., 2010; Shmuel and Leopold, 2008), and their spatiotemporal dependencies recapitulate known task-related patterns and reflect the brain's intrinsic connectivity (Krienen et al., 2014; Smith et al., 2009).

Several cross-sectional studies using rs-fMRI have linked mild cognitive impairment, amyloid pathology, or AD severity to altered connectivity in the so-called default mode network (Buckner et al., 2008; Elman et al., 2016; Greicius et al., 2004; Jiang et al., 2016; Sheline et al., 2010; Sperling et al., 2009; Wang et al., 2013) and visual system (Pan et al., 2017). Recently, connectivity changes have been detected using rs-fMRI in Aβ-positive, but cognitively normal individuals (Sheline et al., 2010). Conversely, network-level disruption has been observed in subjects at high risk for AD but who do not exhibit abnormal amyloid levels (Harrison et al., 2016). Together, these findings suggest that rs-fMRI may be a sensitive marker of neuronal dysfunction and brain connectivity that is independent of protein deposition status across the AD continuum.

Few studies have examined the longitudinal changes in rs-fMRI in the context of known molecular biomarkers of neurological disease (Deng et al., 2016; Hafkemeijer et al., 2017; Ren et al., 2016; Zhan et al., 2016). However, prior work suggests that rs-fMRI may detect disease-specific patterns of connectivity change in patients with AD and frontotemporal lobar degeneration (Hafkemeijer et al., 2017). Moreover, in amyloid positron emission tomography (PET)–positive subjects without dementia, the pattern of glucose metabolism reductions appears to follow a different spatiotemporal distribution than brain atrophy over a 3-year period (Araque Caballero et al., 2015), suggesting that brain function is being affected independent of frank neuronal loss. More recently, functional brain imaging has been used to study the amplitude of low-frequency fluctuations (ALFFs) in gray matter as a relatively pure measure of neuronal activity because it is largely insensitive to breath hold (Zuo et al., 2010) and, therefore, changes in vascular tone. ALFF is also reliable in the presence of motion relative to other rs-fMRI metrics (Yan et al., 2013a). Alterations in ALFF imply changes in brain connectivity (Tomasi et al., 2016). ALFF has good sensitivity to disease and has been reliably monitored in patients with cognitive dysfunction and AD (Han et al., 2011; Li et al., 2012; Pan et al., 2017; Skidmore et al., 2013; Turner et al., 2012; Yan et al., 2013a,b; Zhao et al., 2014; Zou et al., 2015). Recently, a small longitudinal study found that ALFF declines in the striatum of Aβ-positive subjects with mild cognitive impairment (MCI) (Ren et al., 2016).

We conducted a novel longitudinal analysis of the impact of baseline Aβ status on rs-fMRI over a 2-year period using MCI data obtained from an Alzheimer's Disease Neuroimaging Initiative (ADNI) data set (for up-to-date information, see www.adni-info.org). Our analyses focused on a reference region–adjusted variant of ALFF, reference region spontaneous brain activity (SBA-rr). We assessed this sensitive rs-fMRI measurement within an AD-related network-specific coordinate system (NSCS) in relation to cerebrospinal fluid (CSF) and ^{18}F-florbetapir PET Aβ biomarkers. In addition, we determined the extent to which changes in the fluorodeoxyglucose (FDG)-PET signal or cognition correlated with the pattern of longitudinal functional brain changes.

2. Material and methods

2.1. Cohort

Our inclusion criteria, meant to mimic those of a potential intervention trial for early AD, included 62 unique ADNI participants and a total of 288 longitudinal images. Each participant was described by baseline Mini-Mental State Examination score, apolipoprotein E (ApoE) ε4 genotype, age, and sex. All participants had a diagnosis of MCI and a Clinical Dementia Rating-Sum of Boxes (CDR-SB) score ≥0.5 and ≤9. This CDR-SB range captures very mild to mild dementia (O'Bryant et al., 2008). All participants had baseline longitudinal rs-fMRI data and baseline testing for either of 2 amyloid biomarkers, CSF Aβ measurements via the April 2017 release of the University of Pennsylvania CSF biomarkers ADNI data set or baseline amyloid PET via standardized uptake value ratio cutpoint of 1.11 from baseline 18F-florbetapir PET imaging. The CSF cutoff point was defined as Aβ < 977 pg/mL, which maximizes concordance with amyloid PET in the ADNI (Hansson et al., 2018). Based on this information, we classified each subject's Aβ status as positive or negative. Six subjects did not have CSF data and were classified as Aβ+ via 18F-florbetapir PET. There were 8 cases of discrepant Aβ classifications based on CSF versus PET tests. Four individuals were classified as Aβ+ based on CSF criteria and as Aβ− based on 18F-florbetapir PET and 4 were classified as Aβ− based on CSF and as Aβ+ using 18F-florbetapir PET. Discrepant cases were classified as Aβ+. Participant baseline characteristics and temporal distribution of follow-up visits are detailed in Tables 1 and 2, respectively. Each subject included in this study has 3 or more rs-fMRI samples over time.

2.2. T1-weighted MRI, FDG-PET, and rs-fMRI acquisition and processing

Data used in the preparation of this article were obtained from the ADNI database (adni.loni.usc.edu). The ADNI was launched in 2003 as a public-private partnership, led by Principal Investigator Michael W. Weiner, MD. The primary goal of the ADNI has been to test whether serial MRI, PET, other biological markers, and clinical and neuropsychological assessment can be combined to measure the progression of MCI and early AD. We included all usable longitudinal data up to a 2-year duration following baseline from ADNI-2 and ADNI-Go in our analyses.

2.2.1. ADNI data collection

- Rs-fMRI: rs-fMRI was obtained using an echoplanar imaging sequence on a 3.0-Tesla Philips MRI scanner. Acquisition parameters were as follows: 140 timepoints; repetition time,

Table 1
Baseline demographics of the ADNI Aβ-positive (Aβ+) and Aβ-negative (Aβ−) cohorts

Baseline demographics	Aβ− (n = 19)	Aβ+ (n = 43)
Age, mean ± SD, years	70.7 ± 9.0	71.0 ± 6.8
ApoE ε4 copy no., n (%)		
0	16 (84.2)	20 (46.5)
1	2 (10.5)	15 (34.9)
2	1 (5.3)	8 (18.6)
Sex, n (%)		
Female	9 (47.4)	20 (46.5)
Male	10 (52.6)	23 (53.5)
CDR-SB score, mean ± SD	1.2 ± 1.0	1.7 ± 1.0
Clinical diagnosis, n (%)		
AD	0 (0)	0 (0)
CN	0 (0)	0 (0)
EMCI	11 (57.9)	25 (58.1)
LMCI	8 (42.1)	18 (41.9)
SMC	0 (0.0)	0 (0)

See Table 2 for the number of longitudinal follow-up visits included from these same individuals. Three Aβ-negative subjects converted to Aβ-positive over the study period. The designations of "EMCI" versus "LMCI" are determined by ADNI as provided in the adnimerge data set.
Key: Aβ, amyloid beta; AD, Alzheimer's disease; ADNI, Alzheimer's Disease Neuroimaging Initiative; ApoE, apolipoprotein E; CDR-SB, Clinical Dementia Rating-Sum of Boxes; CN, cognitively normal; EMCI, early mild cognitive impairment; LMCI, late mild cognitive impairment; SMC, significant memory complaint.

Table 2
Distribution of the number of longitudinal follow-up visits across the study for the ADNI Aβ-positive (Aβ+) and Aβ-negative (Aβ−) cohorts

Available resting-state data, n (%)	Aβ− (n = 89)	Aβ+ (n = 199)
Baseline	19 (21.3)	43 (21.6)
Month 3	19 (21.3)	46 (23.1)
Month 6	18 (20.2)	40 (20.1)
Month 12	19 (21.3)	36 (18.1)
Month 18	0 (0.0)	1 (0.5)
Month 24	14 (15.7)	33 (16.6)

Key: Aβ, amyloid beta; ADNI, Alzheimer's Disease Neuroimaging Initiative; CDR-SB, Clinical Dementia Rating-Sum of Boxes.

3000 ms; echo time, 30 ms; flip angle, 80°; number of slices, 48; slice thickness, 3.3 mm; spatial resolution, $3 \times 3 \times 3$ mm^3; and in-plane matrix, 64×64.

- T1-weighted MRI: Three-dimensional sagittal magnetization-prepared rapid acquisition with gradient echo images were acquired using Philips Medical Systems 3.0 Tesla scanners. Acquisition parameters were as follows: repetition time, 6.77; echo time, 3.13; flip angle, 9.0°; number of slices, 172; slice thickness, 1.2 mm; spatial resolution, $1 \times 1 \times 1$ mm^3; and in-plane matrix, 256×256.
- FDG-PET: The ADNI acquired FDG-PET scans at over 50 sites on 20 different scanner models with varying resolution. ADNI acquisition and preprocessing steps have been described in detail previously (Jagust et al., 2015). We elected to use the "step 1" preprocessed data, which averages rigidly registered frames in native space. We subsequently registered these images rigidly to the brain-extracted versions of the T1-weighted images for each subject and, by composition, to the ADNI template space discussed in the following. FDG was only available at baseline and 2 years. We also accessed FDG summary variables provided by the ADNI PET Core (Jagust et al., 2015).

2.2.2. Data processing

T1-weighted and rs-fMRI processing steps (Fig. 1) followed methods described previously (Avants et al., 2015). Briefly, we constructed a population-specific group template (Avants et al., 2015) with probabilistic tissue priors and anatomical labels derived from the Desikan-Killiany-Tourville protocol (Klein and Tourville, 2012), an NSCS (Power et al., 2011), and a high-resolution vessel template (Viviani, 2016). It also contained the automated anatomical labeling set (Rolls et al., 2015). This custom template and collection of anatomical labels enabled spatial normalization and prior-based segmentation for each subject and timepoint in the study (Tustison et al., 2014a). We motion-corrected each BOLD image to an iteratively computed time series mean and collected the final transformation parameters for assessment of quality assurance. We also computed nuisance variables within noncortical tissue via CompCor, keeping 10 nuisance predictors (Shirer et al., 2015). We built our longitudinal resting-state analysis using the approach of Shirer et al. because, to our knowledge, theirs is the only available study with clearly identified optimal parameters in a training and testing framework that maximize both reliability as well as diagnostic sensitivity in AD (Shirer et al., 2015). We residualized nuisance variables from the BOLD signal within the cerebrum, performed wavelet filtering (Wink and Roerdink, 2004), and computed ALFF (Pan et al., 2017) as a voxel-wise measurement of SBA-rr. We subsequently aligned the mean BOLD image to the brain-extracted T1-weighted image at each individual timepoint. We then mapped the BOLD data to the group space through a composite transformation. Finally, we indexed the SBA-rr at a priori standardized coordinates (Power et al., 2011). The NSCS was based on a large meta-analysis that defined loci for robust functional effects in the literature. This coordinate system suggests networks of functional specialization in the brain and where one might reliably identify effects despite myriad processing choices (Pernet and Poline, 2015). A subset ($\approx$ 7%) of individual timepoints of resting-state—exhibited excessive motion artifact, based on framewise displacement, were removed from further analysis (n = 15 unique images, not unique subjects). In our analyses, we extended the ALFF measurement using methods that stabilize it longitudinally. Our construct used the original ALFF signal minus the mean ALFF within the cerebellum computed after the custom fMRI preprocessing defined previously. The cerebellar ALFF is a proxy measurement for "DC noise," that is, background scanning and physiological signal not relevant to the AD-related cortical signals of interest. This technique is similar to global signal subtraction (Liu et al., 2017) and only removes a single constant value from each session's overall voxel-wise ALFF measurement. The approach is unbiased with respect to the variables of interest and seeks to cancel or limit noise that may compromise longitudinal assessments of SBA. We tested this processing pipeline using a publicly available data set (Orban et al., 2015) to establish reliability within an aging population at risk for AD (Avants, 2018).

2.3. Computational platform and software

We used R version 3.3.2 ("Sincere Pumpkin Patch") for basic statistical processing and ANTsR version 0.3.3 (Muschelli et al., 2017, submitted; Stone et al., 2016; Tustison et al., 2015) for core image analysis and data organization.

3. Theory/calculation

3.1. Spatial distribution of regions with longitudinal trajectories that differ with Aβ status

Both visual and default networks are sites of early cross-sectional differences in AD, potentially even at the prodromal level (Sheline et al., 2010; Sperling et al., 2009). Our primary analysis focused on whether SBA-rr changes within these networks were impacted by differences in Aβ status. We tested our hypothesis within a subset of ADNI patients with MCI. We included a measurement of SBA-rr within a probabilistic vessel region as a negative control.

We evaluated amyloid-related SBA-rr change, along with its spatial distribution, within these predefined networks using mixed-effects modeling. We tested the model at each of 92 locations within the NSCS that are part of the visual or default network as well as the vessel template. The mixed-effects framework allowed subject-specific longitudinal trajectories to be modeled while controlling for baseline conditions as well as subject- and site-specific random effects (Tan et al., 2013; Verbeke and Fieuws, 2007). The following mixed-effects model captures the potential effect of baseline Aβ status (denoted as Aβ in the following model) over the whole 2-year time window while controlling for baseline SBA:

$$\begin{aligned} \mathrm{SBA}_{\mathrm{change}} \approx \mathrm{SBA}_{\mathrm{base}} + \mathrm{APOE4} + \mathrm{CDRSB.bl} + \mathrm{SEX} + \mathrm{AGE} + \mathrm{FD} \\ + \mathrm{t} + \mathrm{A\beta} + \mathrm{A\beta}:t + (1|\mathrm{PTID}) + (1|\mathrm{SITE}) \end{aligned}$$

Here, t is the time from baseline, FD indicates framewise displacement, and PTID and SITE are patient- and site-specific random effects, respectively. We estimated these models with lme4 (Bates et al., 2015) and significance using lmerTest packages in

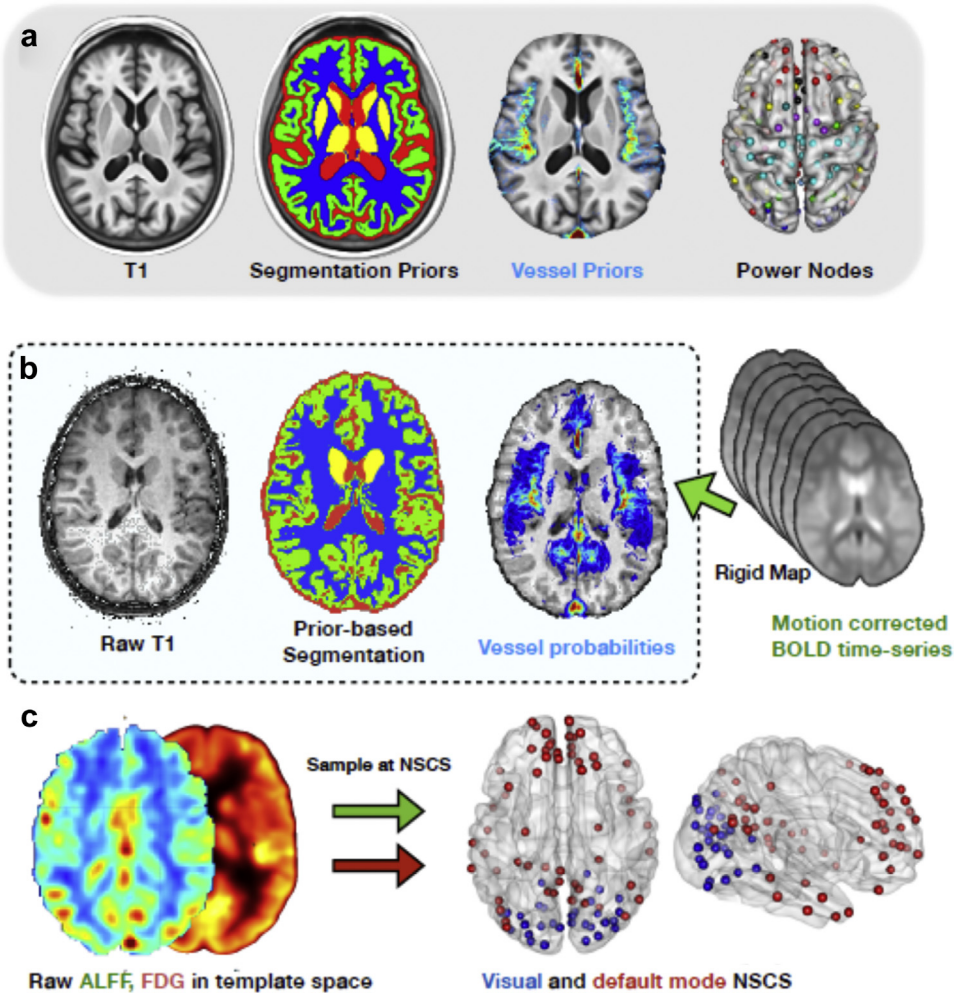

Fig. 1. Overview of the processing pipeline sequence. The template and priors, which guide segmentation and localization of the NSCS in the individual subject's T1-weighted images, are illustrated in (a). Results of T1 processing are illustrated in (b), where we also see how BOLD (and FDG; not shown) images are transformed to the individual subject's T1 space, allowing location of tissue classes, which guides nuisance variable computation. Once modality-specific preprocessing is complete, in (c), we transform the FDG and raw ALFF images into the template space and compute SBA-rr in the NSCS in preparation for final population-level statistics. Abbreviations: ALFF, amplitude of low-frequency fluctuations; BOLD, blood oxygen level–dependent; FDG, fluorodeoxyglucose; SBA-rr, reference region spontaneous brain activity; NSCS, network-specific coordinate system.

R (The R Foundation, 2017). Note that assigning p values to mixed-effects models is a controversial topic, as there is no inherently defined method to calculate degrees of freedom, and thus, several approaches exist for determining p values (Bernal-Rusiel et al., 2013; Luke, 2017). We, therefore, corrected the estimated p values using a conservative Bonferroni method to control for family-wise error. In this analysis, the interaction term Aβ:t is the main predictor of interest for hypothesis testing. Our analysis yielded multiple comparison–controlled empirical p values (q values) for all 92 tests performed across the brain.

3.2. Change in SBA-rr within vessels

We used a high-resolution probabilistic vessel template (Viviani, 2016) to determine whether we see the same effects within a set of voxels likely related to vessels. After mapping the vessel probability atlas to our template space, we computed SBA-rr within only high-probability vessel regions and ran the same statistical model as mentioned previously. If results were not present within the vessel region of interest but were present in the anatomical/network regions of interest, our hypothesis that the signal is a consequence of neuronal activity was supported.

3.3. Comparing rs-fMRI with FDG-PET

Neurovascular coupling is believed to translate the underlying neural activity to a measurable BOLD response. Electrophysiological studies show strong correlations between resting BOLD signal and local field potentials (Scholvinck et al., 2010). However, BOLD measurements may also be influenced by physiological noise, cognitive state, motion, blood flow, blood volume, and metabolism (Caballero-Gaudes and Reynolds, 2017; Hall et al., 2016a; Turner, 2016; Ugurbil, 2016). While our aforementioned processing approach sought to use both prior and data-driven methods to control for these factors, we also compared our data to FDG-PET to further assess our models.

FDG-PET measures the metabolic rate in the brain directly via phosphorylation of glucose metabolism. Several studies have shown that brain FDG signal changes with AD progression (Cerami et al., 2014; Ewers et al., 2013; Kadir et al., 2012; Landau et al., 2011; Lange et al., 2016; Xu et al., 2016). We tested whether glucose

Table 3
Bonferroni-corrected NSCs where Aβ status impacts longitudinal change in SBA-rr

NSC	Cortical region	Brod	Network	Aβ+ decline *t*-value	Aβ+ decline *p*-value
147	L. middle occipital	19	Visual	-3.97	<0.0001
151	L. lingual	18	Visual	-3.93	0.00011
172	L. fusiform	19	Visual	-3.84	0.00015
80	R. middle occipital	39	Default mode	-3.88	0.00013
90	L. precuneus	30	Default mode	-3.90	0.00012
95	**R. precuneus**	**30**	**Default mode**	**-3.79**	**0.00018**
97	R. dorsal superior frontal	9	Default mode	-3.84	0.00015
130	R. angular gyrus	39	Default mode	-4.21	<0.0001

Brod and AAL indicate the putative Brodmann area and AAL region determined by the template. PvalRecall refers to immediate recall; delayed recall was not significant (Tzourio-Mazoyer et al., 2002). The row in bold is the NSC that relates to change in immediate recall.
Key: AAL, automated anatomical labeling; Aβ, amyloid beta; Brod, Brodmann area; L, left; SBA-rr, reference region spontaneous brain activity; NSC, network-specific coordinate; R, right.

metabolism underlies our observed changes in SBA-rr by adding both baseline FDG and change in FDG terms to our original model as follows:

$$SBA_{change} \approx \cdots + FDG_{base} + FDG_{change}$$

These modifications allowed us to determine whether changes in FDG predict change in SBA-rr while controlling for other variables. Each FDG measurement is taken at the same location as the SBA-rr measurement. This model tests for Aβ effects that are significant even after controlling for effects of FDG. We tested this model using both ADNI PET Core summary variables and our own processing, which provided FDG values in the NSCS. As clarified in the following sections, we computed this model for all network-specific coordinates (NSCs) but focused with this secondary FDG model only on regions that were significant in the original SBA-rr model.

3.4. Comparing with cognitive change

Recent work points toward an earlier role for subtle cognitive deficits in the AD biomarker model (Edmonds et al., 2015). Thus, we sought to constrain our interpretation further by assessing whether significant changes in rs-fMRI related to amyloid are also related to change in memory. Immediate and delayed recall memory scores are among the most discriminative clinical measurements available for AD (Estevez-Gonzalez et al., 2003; Haapalinna et al., 2016; Kandel et al., 2015b; Ramanan et al., 2016; Scheff et al., 2013; Wolk et al., 2011). Previous studies have shown that both recall measures may be longitudinally sensitive in AD (Bilgel et al., 2014). We again build on our previous model and test whether our observed changes in SBA-rr related to changes in either immediate or delayed recall (denoted MEM in the equation below):

$$SBA_{change} \approx \text{terms from prior model} + MEM_{base} + MEM_{change} + A\beta : MEM_{change}$$

Just as in the FDG model, this allowed us to determine whether changes in MEM related to changes in SBA-rr while controlling for other variables. We tested the significance of the $A\beta^{*}MEM_{change}$ term in this model to assess whether Aβ status interacts with cognitive change over time to impact SBA_{change}. This strategy tested the multivariate improvement in the model due specifically to memory-related variables.

4. Results

4.1. Spatial distribution of regions with longitudinal trajectories that differ with Aβ status

Following multiple comparisons correction, we identified 8 cortical regions where SBA-rr showed significant changes driven by the difference in longitudinal trajectories between baseline Aβ-positive and Aβ-negative subjects. The pattern of change included default NSCs in both the anterior and posterior portions of the default mode network, as well as in proximal visual regions. Table 3 and Fig. 2 highlight these results in detail.

4.2. Change in SBA-rr within probable vessel regions, FDG, immediate recall, and framewise displacement

We report the results of alternative possible predictors for the longitudinal changes observed, i.e., changes in vasculature, glucose metabolism, and degree of motion during scanning. SBA-rr within the probabilistic vessel template did not show amyloid-related changes over time. The *p* value for the amyloid-time interaction term was >0.8. This indicates that effects detected in other regions are likely to be more specific to neural activity than to changes in non-neuronal signal, such as vascular reactivity. The statistical model applied to SBA-rr within the vessel template did not reach significance.

FDG did not explain sufficient variance to reach significance within the regions detected by rs-fMRI. However, over all tested NSCs in the visual and default networks, FDG did add significant information to the model for 2 NSCs, both part of the visual

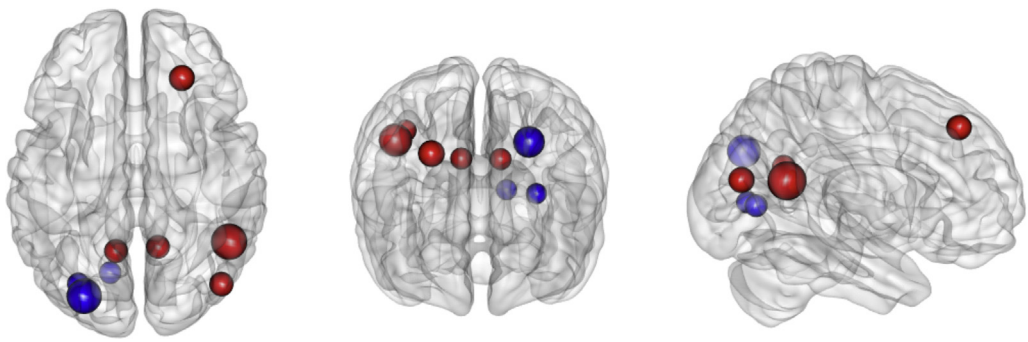

Fig. 2. Spatial distribution of regions with longitudinal trajectories that differ with Aβ status. The blue nodes are associated with visual association cortices, Brodmann areas 18 and 19, while the red coordinates are in the default network including the superior frontal gyrus, precuneus, and angular gyrus. Overall, the effects localized primarily to hub-like heteromodal association areas. A larger radius was associated with greater Bonferroni-corrected significance. Abbreviation: Aβ, amyloid beta.

network. The approximate anatomical regions corresponded to middle occipital gyrus (Montreal Neurological Institute coordinate, −37, 84, 13) and fusiform gyrus (Montreal Neurological Institute coordinate, −27, 59, −9). Thus, changes in glucose metabolism alone are unlikely to explain the findings described here.

Our models for predicting change in SBA-rr measures related to change in immediate recall were significant at a Bonferroni-corrected significance level of 0.05. Delayed recall, in contrast, did not show a relationship at this significance level. As reported in Table 3, the precuneus demonstrated an interaction-based Bonferroni-corrected relationship to change in immediate recall (adjusted $p < 0.05$). We illustrate this effect in Fig. 3 which shows that stable SBA-rr is related to more stable cognition in Aβ-negative subjects; In Aβ-positive subjects, however, reductions in SBA-rr were related to more stable cognitive performance. Relatively few (n = 5) Aβ-negative subjects show decline in the time period studied, whereas roughly half (n = 21) of the Aβ-positive subjects showed decline. This effect may relate either to learning or to cognitive flexibility as a result of the ongoing disease process. Additional false discovery rate–corrected regions also related to immediate recall but were excluded by our initial significance cutoff. To rule out motion as the source of longitudinal group differences, we also examined relationships between important covariates within our model and the mean framewise displacement (FD), a measure of overall motion within each rs-fMRI data set. Mixed-effects models did not identify relationships between baseline CDR-SB, APOE genotype, sex, age, Aβ status, or time with change in FD. However, it is not clear whether patient- or site-specific random effects were relevant for sporadic motion. Thus, we also tested a standard linear regression model that investigated whether FD is impacted by change in APOE genotype, age, change in cognition, Aβ status, or sex. This model showed a small significant relationship of age with FD ($p < 0.03$).

Finally, after finalizing our NSC results, we sought to visualize the overall patterns of change that may be missed by our conservative NSCS. We, thus, performed a dense vertex-wise analysis computing the mixed-effects model for SBA change at every vertex in the cortex. This allowed us to visualize whether there are large expanses of the cortex that show the same or similar patterns of change to our primary results. This exploratory and descriptive result further confirmed the specificity of the findings. Fig. 4 shows the pattern of effects. Few, if any, regions had significant uncorrected p values (selecting 0.001 as a cutoff) outside of the default or visual network.

5. Discussion

The present study integrated longitudinal rs-fMRI, FDG-PET, measurements of episodic memory, and baseline Aβ biomarkers into a single analysis of serial functional change in subjects with MCI. The findings suggest that SBA-rr in baseline Aβ−negative subjects diverges from baseline Aβ−positive subjects over 2 years within subsystems of the default and visual networks, locations in the brain that are both functionally important and impacted by AD. The strongest statistical effects of Aβ in this study isolated to the precuneus and lateral inferior parietal lobes, regions that are well-established functional hubs and form the core of the posterior default network. The results reaffirm the role of the precuneus in AD progression and its concomitant sensitivity to amyloid accumulation (Perrotin et al., 2012), while also reinforcing the hypothesis that AD is, at least in later stages, a network-level disease. It is also notable that while these anatomical-functional regions seem to be impacted in AD patients ahead of cognitive symptoms, they also exhibit longitudinal sensitivity relative to Aβ-negative patients well into the clinically identifiable disease course that was studied here. The visual cortex is highly interconnected anatomically and functionally with key regions that are primary loci of degeneration in AD. In addition, the visual cortex was implicated in some of the earliest rs-fMRI studies in AD wherein cognitively normal Aβ-positive subjects were contrasted against controls (Sheline et al., 2010). A more recent study explored functional biomarkers of AD using rs-fMRI and “found diminished connectivity in the primary visual cortex” both in patients with MCI due to AD and patients with AD (Badhwar et al., 2017), whereas our study identifies longitudinal effects of amyloid positivity using rs-fMRI. In summary, these findings may be unsurprising given that the optic nerve is affected in AD (Sadun and Bassi, 1990), which may also lead to functional alterations downstream potentially distinct from or preceding anatomical cortical alterations.

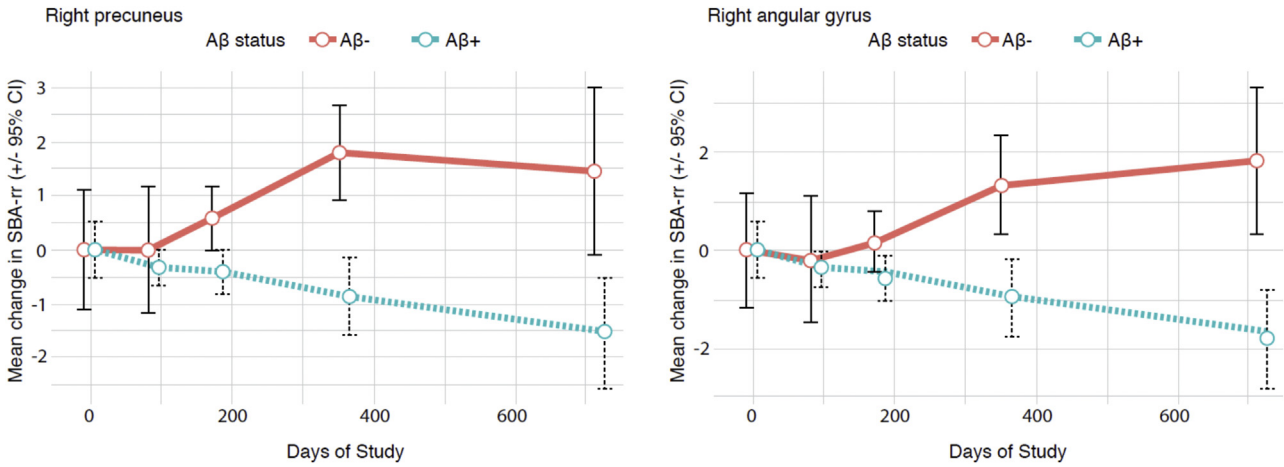

Fig. 3. Longitudinal plots with CIs for 2 representative significant regions, the right precuneus and right angular gyrus. The time series plot represents the change in SBA-rr variables. The overall gap between the Aβ-positive (Aβ+) and Aβ-negative (Aβ−) subjects increased over the time of the study; The precuneus CI suggests high confidence for reduction in Aβ-positive subjects' SBA-rr. The CIs account for repeated measures as described previously (Morey, 2008). Note that the mixed-effects model effectively considers the full-time series for both groups in estimating the likelihood of the difference in trajectories due to amyloid status. See Tables 1 and 2 for the n value at each timepoint. Abbreviations: Aβ, amyloid beta; CI, confidence interval; SBA-rr, reference region spontaneous brain activity.

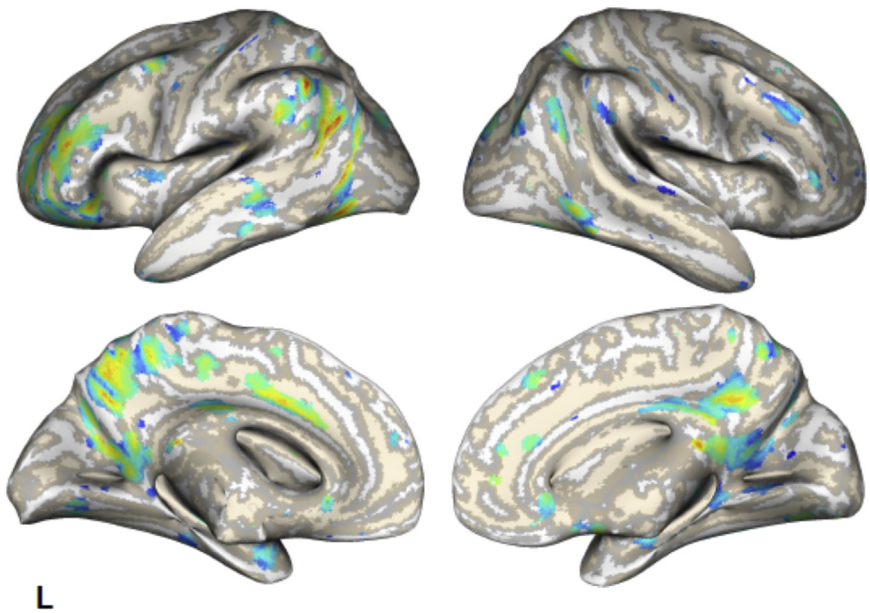

Fig. 4. Uncorrected exploratory vertex-wise analysis results. This figure shows uncorrected p values of <0.001 arising from the SBA-rr change model previously run only at NSCs. The primary effects were in the same direction as that reported at the NSCs and few, if any, results trended in the opposite direction. This further supports the specificity of the NSC findings. Abbreviations: SBA-rr, reference region spontaneous brain activity; NSCs, network-specific coordinates.

5.1. *Aβ and brain function*

Molecular biomarkers were used as a primary outcome measure to constrain our interpretation of the rs-fMRI effects. By considering several supplemental markers, described previously, we argue that observed differences in longitudinal measures of brain activity result from synaptic/neuronal dysfunction, potentially at a network level, related to downstream effects of amyloid pathology. We suggest that the cause of this disruption is linked to the failure of compensatory mechanisms that help combat age-related cognitive decline. This may be due to inflammation or resting alterations in the production or regulation of neurotransmitters, such as glutamate, that are essential for efficient activation and potentially reorganization of cognitive networks. Alternatively, the changes observed here may relate to the disruption of post-synaptic activity by soluble Aβ oligomers (Hu et al., 2008). However, in the absence of a direct molecular marker, we cannot confirm this hypothesis.

Amyloid may alter the SBA-rr trajectory through a variety of physiological mechanisms. SBA-rr is based on ALFF, which computes total power within a physiologically and hardware-limited frequency range. The frequency band is chosen to reflect the components of the BOLD signal that are more likely to be related to neuronal activity within the resting state. Thus, ALFF indexes the local strength of spontaneous fluctuations in local field potentials, which putatively represent the integrated electrophysiological result of synaptic activity (Hutchison et al., 2015; Scholvinck et al., 2010; Shmuel and Leopold, 2008). Even accounting for the specificity of our design and statistical control for confounders, it is possible that these brain activity changes may retain some signal due to a variety of other effects of AD pathology on neurovascular coupling. Fundamentally, AD impacts both neuronal activity and neural connectivity, neurometabolism, and hemodynamics (Iadecola, 2004). Moreover, the entire neuro-glial-vascular unit may be impacted simultaneously in clinically detectable AD (Musiek and Holtzman, 2015). Thus, while evidence supports the synaptic foundation of the BOLD signal, underlying AD pathology has several routes through which it may alter synaptic activity and, consequently, observed SBA-rr.

In addition, the molecular biomarkers on which we rely may relate to different aspects of AD. For instance, CSF may be more sensitive to detecting amyloid pathology earlier in the disease process in comparison to amyloid PET (Bateman et al., 2012). We also included FD in our statistical models to control for the impact of motion. We found only modest effects, especially in comparison to other predictors that are more directly related to the AD phenotype.

5.2. *SBA-rr and cognitive decline*

The precuneus and lateral portions of the default network are areas of elevated resting metabolism relative to the rest of the brain (Cavanna and Trimble, 2006). This pair of regions has been associated with memory encoding (precuneus) (Celone et al., 2006; Miller et al., 2008; Wolk et al., 2011) and retrieval (angular gyrus/lateral occipital lobe) (Bonner et al., 2013; Bonnici et al., 2016). Our results show that longitudinal change in the posterior default network may relate to changes in immediate recall. Change in immediate recall over 2 years was different between Aβ-positive and Aβ-negative subjects (Fig. 5). Aβ-positive subjects with more stable SBA-rr also showed reduced performance over time. Thus, change in SBA-rr may indicate a failure in compensation to the ongoing disease process in Aβ-positive subjects. Moreover, although we controlled for baseline CDR-SB scores and baseline immediate recall in our models, persistent and difficult-to-measure perturbations in the underlying disease stage may explain some variability in both cognitive decline over time and the relationship with SBA-rr. In Aβ-negative subjects, the relationship between these measurements was relatively weaker, which may be the consequence of fewer Aβ-negative subjects showing change in immediate recall over 2 years. Memory tests that are less susceptible to learning effects, longer measurement intervals, or larger sample sizes may be necessary to detect such relationships more reliably. The relationship between SBA-rr and cognitive decline supports the hypothesis that SBA-rr measurement indexes neuronal, as opposed to metabolic, dysfunction. Our results inform the timing and spatial specificity of functional changes within subjects who exhibit clinically

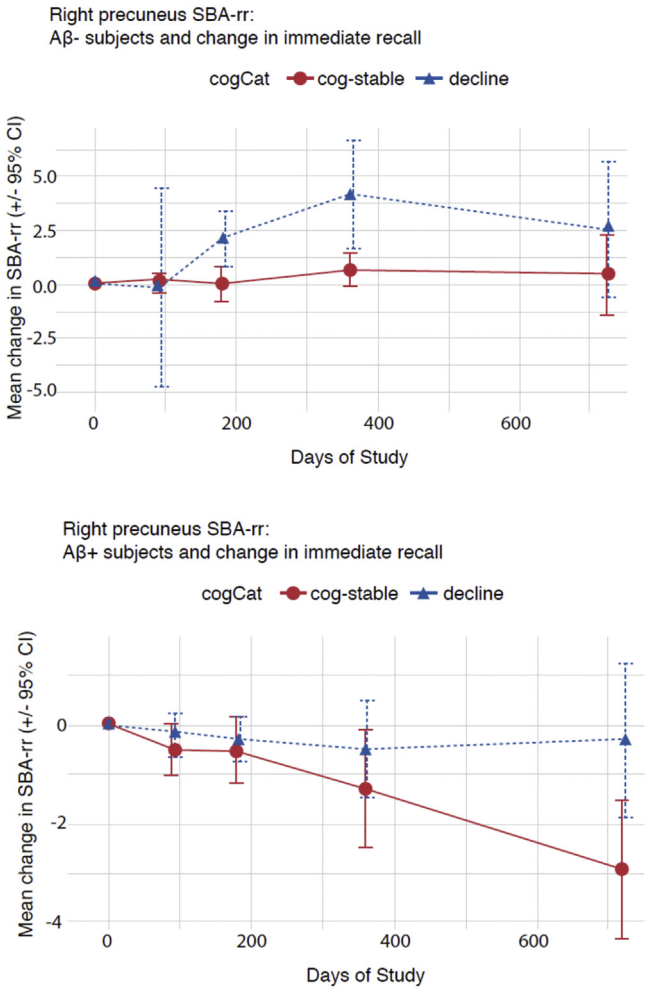

Fig. 5. The interaction between Aβ status and change in cognition. The picture approximates, visually, what the interaction term captures in the statistical model, by categorizing longitudinal change in immediate recall into "stable" and "declining" groups, the latter defined by those who have substantially reduced recall abilities. The interaction is primarily driven by subjects who show relative cognitive stability in immediate recall. Relatively few (n = 5) Aβ-negative (Aβ−) subjects show decline in the time period studied, whereas roughly half (n = 21) of the Aβ-positive (Aβ+) subjects showed decline. This effect may relate to a learning or cognitive flexibility as a result of the ongoing disease process. Abbreviations: Aβ, amyloid beta; CI, confidence interval; SBA-rr, reference region spontaneous brain activity.

detectable cognitive decline and are also Aβ positive. Future work with SBA-rr may refine data-driven staging markers even further, potentially allowing prediction of cognitive decline within specific psychometric domains.

5.3. Predictors of SBA-rr beyond amyloid

We explored the relationships of our longitudinal measurements with other explanatory variables, including FDG-PET and in-scan motion. Neither of these factors explained the notable variance in our proposed longitudinal models over and above baseline Aβ status and other covariates. Although FDG-PET did show sensitivity to Aβ status in other parts of the brain, these effects did not cooccur with those that we found to differ between groups with SBA-rr. The proposed SBA-rr results, therefore, appear to be largely independent of glucose metabolism as well as motion artifact. The results are also spatially localized to anatomical coordinates within AD-related networks, providing additional confidence in these results.[2] While it is possible that cerebral atrophy could explain the SBA-rr alterations, we found no relationship between gray matter content at our candidate NSCs (albeit they were not optimized for assessing atrophy patterns) and Aβ positivity (results not shown).

5.4. Methodological considerations

Our analysis examined the longitudinal changes in regional brain activity using several innovative analytical approaches. First, a cerebellar region was used as a reference against which SBA-rr was measured in other brain areas to capture residual aspects of motion or physiologically related background signal that increases with age (Savalia et al., 2017). The use of a reference region produced measurements that were more stable longitudinally at an individual level and, therefore, more statistically sensitive in serial population studies using mixed-effects models. Second, we implemented a high-dimensional template-based registration (Tustison et al., 2014b) to accurately (at least within the resolution of fMRI) locate the NSCS in each individual anatomical-functional image pair. Third, we sampled functional values specifically within the default and visual networks based on a substantial body of prior work suggesting the sensitivity of these networks to AD-related pathology and used these within a mixed-effects framework. In addition to novel contributions, we leveraged prior work, particularly in establishing reliable fMRI processing approaches in AD (Shirer et al., 2015) and reliable rs-fMRI metrics (Pan et al., 2017), to guide our decision-making in the pipeline design process. This collection of techniques enabled a novel study of the longitudinal changes in rs-fMRI in a cohort with evidence of amyloid pathology based on molecular biomarkers.

5.5. Limitations and future work

A primary concern with BOLD-based studies is the degree to which changes in signal are linked to alterations in underlying neuronal activity. Indeed, the origin of neuro-glial-vascular coupling and its link to BOLD images is an area of active research and debate (Hall et al., 2016b). While Aβ levels may indeed be linked to neurovascular coupling, this study partially addresses these concerns by employing molecular biomarkers of AD neuropathology to define variables of interest. This approach was complemented with informative statistical models to constrain the interpretation by introducing measurements that may index different points in the cascade of AD.

A second limitation of this study is that Aβ status was defined only at baseline, as would occur in an intervention study. However, this static dichotomy does not eliminate the possibility that Aβ-negative subjects converted to Aβ-positive over the study period. Indeed, 2 subjects converted to Aβ-positive in this cohort, which may bias our findings to the statistically conservative side. This study also dichotomizes individuals as Aβ-positive if either CSF Aβ42 or 18F-florbetapir PET measurements were positive. No cognitive impairment score was used in this decision. Such inclusion criteria for determining amyloid positivity may be considered another limitation of the study design. Future work, in larger data sets, will allow more detailed longitudinal studies that may illuminate the dynamics of rs-fMRI as a function of concordant and/or discordant Aβ CSF and PET biomarkers.

[2] We included framewise displacement in our models to check their sensitivity to this parameter and found relatively small effects overall, especially in comparison to other predictors.

The present study had a relatively small number of individuals and timepoints. This is an important concern when considering a disease that evolves over a lifespan and may be impacted by yet unknown hereditary factors. AD is likely more complex when one considers the broader diversity of the population, which will impact brain plasticity during aging, a critical substrate of cognitive reserve. In addition, unknown contributions of secondary pathology to AD biomarker dynamics may be a concern, as some studies suggest that "pure AD" is relatively rare (Toledo et al., 2013). Thus, while we sought to make our analysis specific to Aβ status, it is unclear what tau or vascular pathologies may contribute to our observations. Furthermore, while SBA-rr showed a relatively powerful dynamic response in this short-interval study, it remains to be seen whether rs-fMRI will prove longitudinally sensitive in pharmaceutical intervention studies.

Further work is needed to better characterize the dynamics of the longitudinal changes in AD with greater anatomical and functional detail in cohorts that are more representative of the global population. It will be of critical importance to resolve the timing and interaction of the changes in functional and molecular biomarkers and how these relate to progressive cognitive decline. Emerging data sets such as PREVENT-AD, UK Biobank (Miller et al., 2016), and Lifespan Human Connectome (Fan et al., 2016; Zuo et al., 2017) may provide this opportunity.

6. Conclusion

While there are caveats of using rs-fMRI as a dependent measure, it is a widely available tool to explore functional alterations that may respond more rapidly to changes in disease state compared with structural neuroimaging or other modalities, thereby broadening the characterization of the functional impact of pathology. Indeed, we showed that Aβ status at baseline was linked to change in SBA over time within default and visual networks and that these changes co-occur with domain-specific cognitive decline. Thus, SBA-rr changes are related to specific clinical symptoms and may be independent of glucose metabolism, supporting the hypothesis that positive Aβ status detrimentally impacts spontaneous neuronal activity or, more generally, neurovascular coupling.

Declaration of interest

All authors are or were employed by Biogen. Dr Hargreaves is currently employed by Celgene. Dr Beaver is a shareholder of Biogen, Abbvie, and GSK.

Acknowledgements

Data collection and sharing for this project was funded by the Alzheimer's Disease Neuroimaging Initiative (ADNI) (National Institutes of Health Grant U01 AG024904) and DOD ADNI (Department of Defense award number W81XWH-12-2-0012). The ADNI is funded by the National Institute on Aging, the National Institute of Biomedical Imaging and Bioengineering, and through generous contributions from the following: AbbVie, Alzheimer's Association; Alzheimer's Drug Discovery Foundation; Araclon Biotech; BioClinica, Inc; Biogen; Bristol-Myers Squibb Company; CereSpir, Inc; Cogstate; Eisai Inc; Elan Pharmaceuticals, Inc; Eli Lilly and Company; EuroImmun; F. Hoffmann-La Roche Ltd and its affiliated company Genentech, Inc; Fujirebio; GE Healthcare; IXICO Ltd; Janssen Alzheimer Immunotherapy Research & Development, LLC.; Johnson & Johnson Pharmaceutical Research & Development LLC.; Lumosity; Lundbeck; Merck & Co, Inc; Meso Scale Diagnostics, LLC.; NeuroRx Research; Neurotrack Technologies; Novartis Pharmaceuticals Corporation; Pfizer Inc; Piramal Imaging; Servier; Takeda Pharmaceutical Company; and Transition Therapeutics. The Canadian Institutes of Health Research is providing funds to support ADNI clinical sites in Canada. Private sector contributions are facilitated by the Foundation for the National Institutes of Health (www.fnih.org). The grantee organization is the Northern California Institute for Research and Education, and the study is coordinated by the Alzheimer's Therapeutic Research Institute at the University of Southern California. ADNI data are disseminated by the Laboratory for Neuro Imaging at the University of Southern California. This work was funded by Biogen. Medical writing support and editing for this article was funded by Biogen and was provided by Nucleus Global.

References

Araque Caballero, M.Á., Brendel, M., Delker, A., Ren, J., Rominger, A., Bartenstein, P., Dichgans, M., Weiner, M.W., Ewers, M., Alzheimer's Disease Neuroimaging Initative (ADNI), 2015. Mapping 3-year changes in gray matter and metabolism in Aβ-positive nondemented subjects. Neurobiol. Aging 36, 2913–2924.

Avants, B.B., Duda, J.T., Kilroy, E., Krasileva, K., Jann, K., Kandel, B.T., Tustison, N.J., Yan, L., Jog, M., Smith, R., Wang, Y., Dapretto, M., Wang, D.J., 2015. The pediatric template of brain perfusion. Sci. Data 2, 150003.

Avants, B.B., 2018. Relating high-dimensional structural networks to resting functional connectivity with sparse canonical correlation analysis for neuroimaging. In: Spalletta, G., Piras, F., Gili, T. (Eds.), Brain Morphometry. Neuromethods, vol 136. Humana Press, New York.

Badhwar, A., Tam, A., Dansereau, C., Orban, P., Hoffstaedter, F., Bellec, P., 2017. Resting-state network dysfunction in Alzheimer's disease: a systematic review and meta-analysis. Alzheimers Dement. (Amst) 8, 73–85.

Bateman, R.J., Xiong, C., Benzinger, T.L.S., Fagan, A.M., Goate, A., Fox, N.C., Marcus, D.S., Cairns, N.J., Xie, X., Blazey, T.M., Holtzman, D.M., Santacruz, A., Buckles, V., Oliver, A., Moulder, K., Aisen, P.S., Ghetti, B., Klunk, W.E., McDade, E., Martins, R.N., Masters, C.L., Mayeux, R., Ringman, J.M., Rossor, M.N., Schofield, P.R., Sperling, R.A., Salloway, S., Morris, J.C., Dominantly Inherited Alzheimer Network, 2012. Clinical and biomarker changes in dominantly inherited Alzheimer's disease. N. Engl. J. Med. 367, 795–804.

Bates, D., Mächler, M., Bolker, B.M., Walker, S.C., 2015. Fitting linear mixed-effects models using lme4. J. Stat. Soft. 67, 1–48.

Berenguer, R.G., Monge Argilés, J.A., Ruiz, C.M., Payá, J.S., Blanco Cantó, M.A., Santana, C.L., 2014. Alzheimer disease cerebrospinal fluid biomarkers predict cognitive decline in healthy elderly over 2 years. Alzheimer Dis. Assoc. Disord. 28, 234–238.

Bernal-Rusiel, J.L., Greve, D.N., Reuter, M., Fischl, B., Sabuncu, M.R., Alzheimer's Disease Neuroimaging Initiative, 2013. Statistical analysis of longitudinal neuroimage data with linear mixed effects models. Neuroimage 66, 249–260.

Bilgel, M., An, Y., Lang, A., Prince, J., Ferrucci, L., Jedynak, B., Resnick, S.M., 2014. Trajectories of Alzheimer disease-related cognitive measures in a longitudinal sample. Alzheimers Dement. 10, 735–742.e4.

Bonner, M.F., Peelle, J.E., Cook, P.A., Grossman, M., 2013. Heteromodal conceptual processing in the angular gyrus. Neuroimage 71, 175–186.

Bonnici, H.M., Richter, F.R., Yazar, Y., Simons, J.S., 2016. Multimodal feature integration in the angular gyrus during episodic and semantic retrieval. J. Neurosci. 36, 5462–5471.

Braak, E., Griffing, K., Arai, K., Bohl, J., Bratzke, H., Braak, H., 1999. Neuropathology of Alzheimer's disease: what is new since A. Alzheimer? Eur. Arch. Psychiatry Clin. Neurosci. 249 (Suppl 3), 14–22.

Buckner, R.L., Andrews-Hanna, J.R., Schacter, D.L., 2008. The brain's default network: anatomy, function, and relevance to disease. Ann. N. Y. Acad. Sci. 1124, 1–38.

Caballero-Gaudes, C., Reynolds, R.C., 2017. Methods for cleaning the BOLD fMRI signal. Neuroimage 154, 128–149.

Cavanna, A.E., Trimble, M.R., 2006. The precuneus: a review of its functional anatomy and behavioural correlates. Brain 129, 564–583.

Cavedo, E., Lista, S., Khachaturian, Z., Aisen, P., Amouyel, P., Herholz, K., Jack Jr., C.R., Sperling, R., Cummings, J., Blennow, K., O'Bryant, S., Frisoni, G.B., Khachaturian, A., Kivipelto, M., Klunk, W., Broich, K., Andrieu, S., de Schotten, M.T., Mangin, J.F., Lammertsma, A.A., Johnson, K., Teipel, S., Drzezga, A., Bokde, A., Colliot, O., Bakardjian, H., Zetterberg, H., Dubois, B., Vellas, B., Schneider, L.S., Hampel, H., 2014. The road ahead to cure Alzheimer's disease: development of biological markers and neuroimaging methods for prevention trials across all stages and target populations. J. Prev. Alzheimers Dis. 1, 181–202.

Celone, K.A., Calhoun, V.D., Dickerson, B.C., Atri, A., Chua, E.F., Miller, S.L., DePeau, K., Rentz, D.M., Selkoe, D.J., Blacker, D., Albert, M.S., Sperling, R.A., 2006. Alterations in memory networks in mild cognitive impairment and Alzheimer's disease: an independent component analysis. J. Neurosci. 26, 10222–10231.

Cerami, C., Della Rosa, P.A., Magnani, G., Santangelo, R., Marcone, A., Cappa, S.F., Perani, D., 2014. Brain metabolic maps in mild cognitive impairment predict heterogeneity of progression to dementia. Neuroimage Clin. 7, 187–194.

Choo, I.H., Ni, R., Schöll, M., Wall, A., Almkvist, O., Nordberg, A., 2013. Combination of 18F-FDG PET and cerebrospinal fluid biomarkers as a better predictor of the progression to Alzheimer's disease in mild cognitive impairment patients. J. Alzheimers Dis. 33, 929–939.

Degerman Gunnarsson, M., Ingelsson, M., Blennow, K., Basun, H., Lannfelt, L., Kilander, L., 2016. High tau levels in cerebrospinal fluid predict nursing home placement and rapid progression in Alzheimer's disease. Alzheimers Res. Ther. 8, 22.

Deng, Y., Liu, K., Shi, L., Lei, Y., Liang, P., Li, K., Chu, W.C., Wang, D., Alzheimer's Disease Neuroimaging Initiative, 2016. Identifying the alteration patterns of brain functional connectivity in progressive mild cognitive impairment patients: a longitudinal whole-brain voxel-wise degree analysis. Front. Aging Neurosci. 8, 195.

Dubois, B., Hampel, H., Feldman, H.H., Scheltens, P., Aisen, P., Andrieu, S., Bakardjian, H., Benali, H., Bertram, L., Blennow, K., Broich, K., Cavedo, E., Crutch, S., Dartigues, J.F., Duyckaerts, C., Epelbaum, S., Frisoni, G.B., Gauthier, S., Genthon, R., Gouw, A.A., Habert, M.O., Holtzman, D.M., Kivipelto, M., Lista, S., Molinuevo, J.L., O'Bryant, S.E., Rabinovici, G.D., Rowe, C., Salloway, S., Schneider, L.S., Sperling, R., Teichmann, M., Carrillo, M.C., Cummings, J., Jack Jr., C.R., Proceedings of the Meeting of the International Working Group (IWG) and the American Alzheimer's Association on "The Preclinical State of AD"; July 23, 2015; Washington DC, USA, 2016. Preclinical Alzheimer's disease: definition, natural history, and diagnostic criteria. Alzheimers Dement. 12, 292–323.

Edmonds, E.C., Delano-Wood, L., Galasko, D.R., Salmon, D.P., Bondi, M.W., Alzheimer's Disease Neuroimaging Initiative, 2015. Subtle cognitive decline and biomarker staging in preclinical Alzheimer's disease. J. Alzheimers Dis. 47, 231–242.

Egli, S.C., Hirni, D.I., Taylor, K.I., Berres, M., Regeniter, A., Gass, A., Monsch, A.U., Sollberger, M., 2015. Varying strength of cognitive markers and biomarkers to predict conversion and cognitive decline in an early-stage-enriched mild cognitive impairment sample. J. Alzheimers Dis. 44, 625–633.

Elman, J.A., Madison, C.M., Baker, S.L., Vogel, J.W., Marks, S.M., Crowley, S., O'Neil, J.P., Jagust, W.J., 2016. Effects of beta-amyloid on resting state functional connectivity within and between networks reflect known patterns of regional vulnerability. Cereb. Cortex 26, 695–707.

Ennis, G.E., An, Y., Resnick, S.M., Ferrucci, L., O'Brien, R.J., Moffat, S.D., 2017. Long-term cortisol measures predict Alzheimer disease risk. Neurology 88, 371–378.

Estévez-González, A., Kulisevsky, J., Boltes, A., Otermin, P., Garcia-Sánchez, C., 2003. Rey verbal learning test is a useful tool for differential diagnosis in the preclinical phase of Alzheimer's disease: comparison with mild cognitive impairment and normal aging. Int. J. Geriatr. Psychiatry 18, 1021–1028.

Ewers, M., Brendel, M., Rizk-Jackson, A., Rominger, A., Bartenstein, P., Schuff, N., Weiner, M.W., Alzheimer's Disease Neuroimaging Initiative (ADNI), 2013. Reduced FDG-PET brain metabolism and executive function predict clinical progression in elderly healthy subjects. Neuroimage Clin. 4, 45–52.

Fan, Q., Witzel, T., Nummenmaa, A., Van Dijk, K.R., Van Horn, J.D., Drews, M.K., Somerville, L.H., Sheridan, M.A., Santillana, R.M., Snyder, J., Hedden, T., Shaw, E.E., Hollinshead, M.O., Renvall, V., Zanzonico, R., Keil, B., Cauley, S., Polimeni, J.R., Tisdall, D., Buckner, R.L., Wedeen, V.J., Wald, L.L., Toga, A.W., Rosen, B.R., 2016. MGH-USC Human Connectome Project datasets with ultra-high b-value diffusion MRI. Neuroimage 124, 1108–1114.

Fox, M.D., Raichle, M.E., 2007. Spontaneous fluctuations in brain activity observed with functional magnetic resonance imaging. Nat. Rev. Neurosci. 8, 700–711.

Greicius, M.D., Srivastava, G., Reiss, A.L., Menon, V., 2004. Default-mode network activity distinguishes Alzheimer's disease from healthy aging: evidence from functional MRI. Proc. Natl. Acad. Sci. U. S. A. 101, 4637–4642.

Haapalinna, F., Paajanen, T., Penttinen, J., Kokki, H., Kokki, M., Koivisto, A.M., Hartikainen, P., Solje, E., Hänninen, T., Remes, A.M., Herukka, S.K., 2016. Low cerebrospinal fluid amyloid-beta concentration is associated with poorer delayed memory recall in women. Dement. Geriatr. Cogn. Dis. Extra 6, 303–312.

Hafkemeijer, A., Möller, C., Dopper, E.G., Jiskoot, L.C., van den Berg-Huysmans, A.A., van Swieten, J.C., van der Flier, W.M., Vrenken, H., Pijnenburg, Y.A., Barkhof, F., Scheltens, P., van der Grond, J., Rombouts, S.A., 2017. A longitudinal study on resting state functional connectivity in behavioral variant frontotemporal dementia and Alzheimer's disease. J. Alzheimers Dis. 55, 521–537.

Hall, C.N., Howarth, C., Kurth-Nelson, Z., Mishra, A., 2016. Interpreting BOLD: towards a dialogue between cognitive and cellular neuroscience. Philos. Trans. R. Soc. Lond. B. Biol. Sci. 371. https://doi.org/10.1098/rstb.2015.0348.

Hall, J.R., Wiechmann, A.R., Johnson, L.A., Edwards, M., Barber, R.C., Winter, A.S., Singh, M., O'Bryant, S.E., 2013. Biomarkers of vascular risk, systemic inflammation, and microvascular pathology and neuropsychiatric symptoms in Alzheimer's disease. J. Alzheimers Dis. 35, 363–371.

Han, Y., Wang, J., Zhao, Z., Min, B., Lu, J., Li, K., He, Y., Jia, J., 2011. Frequency-dependent changes in the amplitude of low-frequency fluctuations in amnestic mild cognitive impairment: a resting-state fMRI study. Neuroimage 55, 287–295.

Hansson, O., Seibyl, J., Stomrud, E., Zetterberg, H., Trojanowski, J.Q., Bittner, T., Lifke, V., Corradini, V., Eichenlaub, U., Batrla, R., Buck, K., Zink, K., Rabe, C., Blennow, K., Shaw, L.M., Swedish BioFINDER study group, 2018. Alzheimer's Disease Neuroimaging Initiative, CSF biomarkers of Alzheimer's disease concord with amyloid-β PET and predict clinical progression: A study of fully automated immunoassays in BioFINDER and ADNI cohorts. Alzheimers Dement 14, 1470–1481.

Hardy, J., Selkoe, D.J., 2002. The amyloid hypothesis of Alzheimer's disease: progress and problems on the road to therapeutics. Science 297, 353–356.

Harrison, T.M., Burggren, A.C., Small, G.W., Bookheimer, S.Y., 2016. Altered memory-related functional connectivity of the anterior and posterior hippocampus in older adults at increased genetic risk for Alzheimer's disease. Hum. Brain Mapp. 37, 366–380.

Hu, N.W., Smith, I.M., Walsh, D.M., Rowan, M.J., 2008. Soluble amyloid-beta peptides potently disrupt hippocampal synaptic plasticity in the absence of cerebrovascular dysfunction in vivo. Brain 131, 2414–2424.

Hutchison, R.M., Hashemi, N., Gati, J.S., Menon, R.S., Everling, S., 2015. Electrophysiological signatures of spontaneous BOLD fluctuations in macaque prefrontal cortex. Neuroimage 113, 257–267.

Iadecola, C., 2004. Neurovascular regulation in the normal brain and in Alzheimer's disease. Nat. Rev. Neurosci. 5, 347–360.

Iturria-Medina, Y., Sotero, R.C., Toussaint, P.J., Mateos-Pérez, J.M., Evans, A.C., Alzheimer's Disease Neuroimaging Initiative, 2016. Early role of vascular dysregulation on late-onset Alzheimer's disease based on multifactorial data-driven analysis. Nat. Commun. 7, 11934.

Jack Jr., C.R., Holtzman, D.M., 2013. Biomarker modeling of Alzheimer's disease. Neuron 80, 1347–1358.

Jack Jr., C.R., Knopman, D.S., Jagust, W.J., Shaw, L.M., Aisen, P.S., Weiner, M.W., Petersen, R.C., Trojanowski, J.Q., 2010. Hypothetical model of dynamic biomarkers of the Alzheimer's pathological cascade. Lancet Neurol. 9, 119–128.

Jack Jr., C.R., Lowe, V.J., Weigand, S.D., Wiste, H.J., Senjem, M.L., Knopman, D.S., Shiung, M.M., Gunter, J.L., Boeve, B.F., Kemp, B.J., Weiner, M., Petersen, R.C., Alzheimer's Disease Neuroimaging Initiative, 2009. Serial PIB and MRI in normal, mild cognitive impairment and Alzheimer's disease: implications for sequence of pathological events in Alzheimer's disease. Brain 132, 1355–1365.

Jagust, W.J., Landau, S.M., Koeppe, R.A., Reiman, E.M., Chen, K., Mathis, C.A., Price, J.C., Foster, N.L., Wang, A.Y., 2015. The Alzheimer's disease neuroimaging Initiative 2 PET core: 2015. Alzheimers Dement. 11, 757–771.

Jiang, Y., Huang, H., Abner, E., Broster, L.S., Jicha, G.A., Schmitt, F.A., Kryscio, R., Andersen, A., Powell, D., Van Eldik, L., Gold, B.T., Nelson, P.T., Smith, C., Ding, M., 2016. Alzheimer's biomarkers are correlated with brain connectivity in older adults differentially during resting and task states. Front. Aging Neurosci. 8, 15.

Kadir, A., Almkvist, O., Forsberg, A., Wall, A., Engler, H., Langstrom, B., Nordberg, A., 2012. Dynamic changes in PET amyloid and FDG imaging at different stages of Alzheimer's disease. Neurobiol. Aging 33, 198.e1–198.e14.

Kandel, B.M., Avants, B.B., Gee, J.C., Arnold, S.E., Wolk, D.A., Alzheimer's Disease Neuroimaging Initiative, 2015a. Neuropsychological testing predicts cerebrospinal fluid amyloid-β in mild cognitive impairment. J. Alzheimers Dis. 46, 901–912.

Kandel, B.M., Avants, B.B., Gee, J.C., McMillan, C.T., Erus, G., Doshi, J., Davatzikos, C., Wolk, D.A., 2016. White matter hyperintensities are more highly associated with preclinical Alzheimer's disease than imaging and cognitive markers of neurodegeneration. Alzheimers Dement. (Amst) 4, 18–27.

Kandel, B.M., Wang, D.J., Gee, J.C., Avants, B.B., 2015b. Eigenanatomy: sparse dimensionality reduction for multi-modal medical image analysis. Methods 73, 43–53.

Klein, A., Tourville, J., 2012. 101 Labeled brain images and a consistent human cortical labeling protocol. Front. Neurosci. 6, 171.

Krienen, F.M., Yeo, B.T., Buckner, R.L., 2014. Reconfigurable task-dependent functional coupling modes cluster around a core functional architecture. Philos. Trans. R. Soc. Lond. B. Biol. Sci. 369. https://doi.org/10.1098/rstb.2013.0526.

Landau, S.M., Harvey, D., Madison, C.M., Koeppe, R.A., Reiman, E.M., Foster, N.L., Weiner, M.W., Jagust, W.J., Alzheimer's Disease Neuroimaging Initiative, 2011. Associations between cognitive, functional, and FDG-PET measures of decline in AD and MCI. Neurobiol. Aging 32, 1207–1218.

Lange, C., Suppa, P., Frings, L., Brenner, W., Spies, L., Buchert, R., 2016. Optimization of statistical single subject analysis of brain FDG PET for the prognosis of mild cognitive impairment-to-Alzheimer's disease conversion. J. Alzheimers Dis. 49, 945–959.

Li, Z., Kadivar, A., Pluta, J., Dunlop, J., Wang, Z., 2012. Test-retest stability analysis of resting brain activity revealed by blood oxygen level-dependent functional MRI. J. Magn. Reson. Imaging 36, 344–354.

Liu, T.T., Nalci, A., Falahpour, M., 2017. The global signal in fMRI: nuisance or information? Neuroimage 150, 213–229.

Luke, S.G., 2017. Evaluating significance in linear mixed-effects models in R. Behav. Res. Methods 49, 1494–1502.

Mattsson, N., Insel, P.S., Donohue, M., Landau, S., Jagust, W.J., Shaw, L.M., Trojanowski, J.Q., Zetterberg, H., Blennow, K., Weiner, M.W., Alzheimer's Disease Neuroimaging Initiative, 2015. Independent information from cerebrospinal fluid amyloid-β and florbetapir imaging in Alzheimer's disease. Brain 138, 772–783.

Mazzeo, S., Santangelo, R., Bernasconi, M.P., Cecchetti, G., Fiorino, A., Pinto, P., Passerini, G., Falautano, M., Comi, G., Magnani, G., 2016. Combining cerebrospinal fluid biomarkers and neuropsychological assessment: a simple and cost-effective algorithm to predict the progression from mild cognitive impairment to Alzheimer's disease dementia. J. Alzheimers Dis. 54, 1495–1508.

Miller, K.L., Alfaro-Almagro, F., Bangerter, N.K., Thomas, D.L., Yacoub, E., Xu, J., Bartsch, A.J., Jbabdi, S., Sotiropoulos, S.N., Andersson, J.L., Griffanti, L., Douaud, G., Okell, T.W., Weale, P., Dragonu, I., Garratt, S., Hudson, S., Collins, R., Jenkinson, M., Matthews, P.M., Smith, S.M., 2016. Multimodal population brain imaging in the UK Biobank prospective epidemiological study. Nat. Neurosci. 19, 1523–1536.

Miller, S.L., Celone, K., DePeau, K., Diamond, E., Dickerson, B.C., Rentz, D., Pihlajamäki, M., Sperling, R.A., 2008. Age-related memory impairment associated with loss of parietal deactivation but preserved hippocampal activation. Proc. Natl. Acad. Sci. U. S. A. 105, 2181–2186.

Morey, R., 2008. Confidence intervals from normalized data: a correction to Cousineau (2005). Tutor. Quant. Methods Psychol. 4, 61–64.

Muschelli, J., Fortin, J., Gherman, A., Avants, B., Whitcherd, B., Caffo, B.S., Crainiceanua, C.M., 2018 Jan 6. Neuroconductor: An R Platform for

Neuroimaging. Biostatistics. https://doi.org/10.1093/biostatistics/kxx068 [Epub ahead of print].
Musiek, E.S., Holtzman, D.M., 2015. Three dimensions of the amyloid hypothesis: time, space and 'wingmen. Nat. Neurosci. 18, 800–806.
O'Bryant, S.E., Waring, S.C., Cullum, C.M., Hall, J., Lacritz, L., Massman, P.J., Lupo, P.J., Reisch, J.S., Doody, R., Texas Alzheimer's Research Consortium, 2008. Staging dementia using clinical dementia rating scale Sum of Boxes scores: a Texas Alzheimer's research Consortium study. Arch. Neurol. 65, 1091–1095.
Orban, P., Madjar, C., Savard, M., Dansereau, C., Tam, A., Das, S., Evans, A.C., Rosa-Neto, P., Breitner, J.C., Bellec, P., PREVENT-AD Research Group, 2015. Test-retest resting-state fMRI in healthy elderly persons with a family history of Alzheimer's disease. Sci. Data 2, 150043.
Pan, P., Zhu, L., Yu, T., Shi, H., Zhang, B., Qin, R., Zhu, X., Qian, L., Zhao, H., Zhou, H., Xu, Y., 2017. Aberrant spontaneous low-frequency brain activity in amnestic mild cognitive impairment: a meta-analysis of resting-state fMRI studies. Ageing Res. Rev. 35, 12–21.
Pernet, C., Poline, J.B., 2015. Improving functional magnetic resonance imaging reproducibility. Gigascience 4, 15.
Perrotin, A., Mormino, E.C., Madison, C.M., Hayenga, A.O., Jagust, W.J., 2012. Subjective cognition and amyloid deposition imaging: a Pittsburgh Compound B positron emission tomography study in normal elderly individuals. Arch. Neurol. 69, 223–229.
Portelius, E., Zetterberg, H., Skillbäck, T., Törnqvist, U., Andreasson, U., Trojanowski, J.Q., Weiner, M.W., Shaw, L.M., Mattsson, N., Blennow, K., Alzheimer's Disease Neuroimaging Initiative, 2015. Cerebrospinal fluid neurogranin: relation to cognition and neurodegeneration in Alzheimer's disease. Brain 138, 3373–3385.
Power, J.D., Cohen, A.L., Nelson, S.M., Wig, G.S., Barnes, K.A., Church, J.A., Vogel, A.C., Laumann, T.O., Miezin, F.M., Schlaggar, B.L., Petersen, S.E., 2011. Functional network organization of the human brain. Neuron 72, 665–678.
Ramanan, S., Flanagan, E., Leyton, C.E., Villemagne, V.L., Rowe, C.C., Hodges, J.R., Hornberger, M., 2016. Non-verbal episodic memory deficits in primary progressive aphasias are highly predictive of underlying amyloid pathology. J. Alzheimers Dis. 51, 367–376.
Ren, P., Lo, R.Y., Chapman, B.P., Mapstone, M., Porsteinsson, A., Lin, F., Alzheimer's Disease Neuroimaging Initiative, 2016. Longitudinal alteration of intrinsic brain activity in the striatum in mild cognitive impairment. J. Alzheimers Dis. 54, 69–78.
Rolls, E.T., Joliot, M., Tzourio-Mazoyer, N., 2015. Implementation of a new parcellation of the orbitofrontal cortex in the automated anatomical labeling atlas. Neuroimage 122, 1–5.
Sadun, A.A., Bassi, C.J., 1990. Optic nerve damage in Alzheimer's disease. Ophthalmology 97, 9–17.
Savalia, N.K., Agres, P.F., Chan, M.Y., Feczko, E.J., Kennedy, K.M., Wig, G.S., 2017. Motion-related artifacts in structural brain images revealed with independent estimates of in-scanner head motion. Hum. Brain Mapp. 38, 472–492.
Scheff, S.W., Price, D.A., Schmitt, F.A., Roberts, K.N., Ikonomovic, M.D., Mufson, E.J., 2013. Synapse stability in the precuneus early in the progression of Alzheimer's disease. J. Alzheimers Dis. 35, 599–609.
Schölvinck, M.L., Maier, A., Ye, F.Q., Duyn, J.H., Leopold, D.A., 2010. Neural basis of global resting-state fMRI activity. Proc. Natl. Acad. Sci. U. S. A. 107, 10238–10243.
Sheline, Y.I., Raichle, M.E., Snyder, A.Z., Morris, J.C., Head, D., Wang, S., Mintun, M.A., 2010. Amyloid plaques disrupt resting state default mode network connectivity in cognitively normal elderly. Biol. Psychiatry 67, 584–587.
Shirer, W.R., Jiang, H., Price, C.M., Ng, B., Greicius, M.D., 2015. Optimization of rs-fMRI pre-processing for enhanced signal-noise separation, test-retest reliability, and group discrimination. Neuroimage 117, 67–79.
Shmuel, A., Leopold, D.A., 2008. Neuronal correlates of spontaneous fluctuations in fMRI signals in monkey visual cortex: implications for functional connectivity at rest. Hum. Brain Mapp. 29, 751–761.
Skidmore, F.M., Yang, M., Baxter, L., von Deneen, K., Collingwood, J., He, G., Tandon, R., Korenkevych, D., Savenkov, A., Heilman, K.M., Gold, M., Liu, Y., 2013. Apathy, depression, and motor symptoms have distinct and separable resting activity patterns in idiopathic Parkinson disease. Neuroimage 81, 484–495.
Smith, S.M., Fox, P.T., Miller, K.L., Glahn, D.C., Fox, P.M., Mackay, C.E., Filippini, N., Watkins, K.E., Toro, R., Laird, A.R., Beckmann, C.F., 2009. Correspondence of the brain's functional architecture during activation and rest. Proc. Natl. Acad. Sci. U. S. A. 106, 13040–13045.
Soldan, A., Pettigrew, C., Li, S., Wang, M.C., Moghekar, A., Selnes, O.A., Albert, M., O'Brien, R., BIOCARD Research Team, 2013. Relationship of cognitive reserve and cerebrospinal fluid biomarkers to the emergence of clinical symptoms in preclinical Alzheimer's disease. Neurobiol. Aging 34, 2827–2834.
Sperling, R.A., Laviolette, P.S., O'Keefe, K., O'Brien, J., Rentz, D.M., Pihlajamaki, M., Marshall, G., Hyman, B.T., Selkoe, D.J., Hedden, T., Buckner, R.L., Becker, J.A., Johnson, K.A., 2009. Amyloid deposition is associated with impaired default network function in older persons without dementia. Neuron 63, 178–188.
Stone, J.R., Wilde, E.A., Taylor, B.A., Tate, D.F., Levin, H., Bigler, E.D., Scheibel, R.S., Newsome, M.R., Mayer, A.R., Abildskov, T., Black, G.M., Lennon, M.J., York, G.E., Agarwal, R., DeVillasante, J., Ritter, J.L., Walker, P.B., Ahlers, S.T., Tustison, N.J., 2016. Supervised learning technique for the automated identification of white matter hyperintensities in traumatic brain injury. Brain Inj. 30, 1458–1468.
Tan, K.S., Libon, D.J., Rascovsky, K., Grossman, M., Xie, S.X., 2013. Differential longitudinal decline on the Mini-Mental State Examination in frontotemporal lobar degeneration and Alzheimer disease. Alzheimer Dis. Assoc. Disord. 27, 310–315.
Taylor, A.N.W., Kambeitz-Ilankovic, L., Gesierich, B., Simon-Vermot, L., Franzmeier, N., Araque Caballero, M.Á., Müller, S., Hesheng, L., Ertl-Wagner, B., Bürger, K., Weiner, M.W., Dichgans, M., Duering, M., Ewers, M., Alzheimer's Disease Neuroimaging Initiative (ADNI), 2017. Tract-specific white matter hyperintensities disrupt neural network function in Alzheimer's disease. Alzheimers Dement. 13, 225–235.
The R Foundation, 2017. The R Project for Statistical Computing.
Toledo, J.B., Bjerke, M., Da, X., Landau, S.M., Foster, N.L., Jagust, W., Jack Jr., C., Weiner, M., Davatzikos, C., Shaw, L.M., Trojanowski, J.Q., Alzheimer's Disease Neuroimaging Initiative Investigators, 2015. Nonlinear association between cerebrospinal fluid and florbetapir F-18 β-amyloid measures across the spectrum of Alzheimer disease. JAMA Neurol. 72, 571–581.
Toledo, J.B., Cairns, N.J., Da, X., Chen, K., Carter, D., Fleisher, A., Householder, E., Ayutyanont, N., Roontiva, A., Bauer, R.J., Eisen, P., Shaw, L.M., Davatzikos, C., Weiner, M.W., Reiman, E.M., Morris, J.C., Trojanowski, J.Q., Alzheimer's Disease Neuroimaging Initiative (ADNI), 2013. Clinical and multimodal biomarker correlates of ADNI neuropathological findings. Acta Neuropathol. Commun. 1, 65.
Toledo, J.B., Da, X., Weiner, M.W., Wolk, D.A., Xie, S.X., Arnold, S.E., Davatzikos, C., Shaw, L.M., Trojanowski, J.Q., Alzheimer's Disease Neuroimaging Initiative, 2014. CSF Apo-E levels associate with cognitive decline and MRI changes. Acta Neuropathol. 127, 621–632.
Tomasi, D., Shokri-Kojori, E., Volkow, N.D., 2016. Temporal changes in local functional connectivity density reflect the temporal variability of the amplitude of low frequency fluctuations in gray matter. PLoS One 11, e0154407.
Turner, J.A., Chen, H., Mathalon, D.H., Allen, E.A., Mayer, A.R., Abbott, C.C., Calhoun, V.D., Bustillo, J., 2012. Reliability of the amplitude of low-frequency fluctuations in resting state fMRI in chronic schizophrenia. Psychiatry Res. 201, 253–255.
Turner, R., 2016. Uses, misuses, new uses and fundamental limitations of magnetic resonance imaging in cognitive science. Philos. Trans. R. Soc. Lond. B. Biol. Sci. 371. https://doi.org/10.1098/rstb.2015.0349.
Tustison, N.J., Cook, P.A., Klein, A., Song, G., Das, S.R., Duda, J.T., Kandel, B.M., van Strien, N., Stone, J.R., Gee, J.C., Avants, B.B., 2014. Large-scale evaluation of ANTs and FreeSurfer cortical thickness measurements. Neuroimage 99, 166–179.
Tustison, N.J., Shrinidhi, K.L., Wintermark, M., Durst, C.R., Kandel, B.M., Gee, J.C., Grossman, M.C., Avants, B.B., 2015. Optimal symmetric multimodal templates and concatenated random forests for supervised brain tumor segmentation (simplified) with ANTsR. Neuroinformatics 13, 209–225.
Tzourio-Mazoyer, N., Landeau, B., Papathanassiou, D., Crivello, F., Etard, O., Delcroix, N., Mazoyer, B., Joliot, M., 2002. Automated anatomical labeling of activations in SPM using a macroscopic anatomical parcellation of the MNI MRI single-subject brain. Neuroimage 15, 273–289.
Ugurbil, K., 2016. What is feasible with imaging human brain function and connectivity using functional magnetic resonance imaging. Philos. Trans. R. Soc. Lond. B. Biol. Sci. 371. https://doi.org/10.1098/rstb.2015.0361.
Verbeke, G., Fieuws, S., 2007. The effect of miss-specified baseline characteristics on inference for longitudinal trends in linear mixed models. Biostatistics 8, 772–783.
Viviani, R., 2016. A digital atlas of middle to large brain vessels and their relation to cortical and subcortical structures. Front. Neuroanat. 10, 12.
Wang, L., Brier, M.R., Snyder, A.Z., Thomas, J.B., Fagan, A.M., Xiong, C., Benzinger, T.L., Holtzman, D.M., Morris, J.C., Ances, B.M., 2013. Cerebrospinal fluid Aβ42, phosphorylated Tau181, and resting-state functional connectivity. JAMA Neurol. 70, 1242–1248.
Wink, A.M., Roerdink, J.B., 2004. Denoising functional MR images: a comparison of wavelet denoising and Gaussian smoothing. IEEE Trans. Med. Imaging 23, 374–387.
Wolk, D.A., Dickerson, B.C., Alzheimer's Disease Neuroimaging Initiative, 2011. Fractionating verbal episodic memory in Alzheimer's disease. Neuroimage 54, 1530–1539.
Xu, L., Wu, X., Li, R., Chen, K., Long, Z., Zhang, J., Guo, X., Yao, L., Alzheimer's Disease Neuroimaging Initiative, 2016. Prediction of progressive mild cognitive impairment by multi-modal neuroimaging biomarkers. J. Alzheimers Dis. 51, 1045–1056.
Yan, C.G., Cheung, B., Kelly, C., Colcombe, S., Craddock, R.C., Di Martino, A., Li, Q., Zuo, X.N., Castellanos, F.X., Milham, M.P., 2013a. A comprehensive assessment of regional variation in the impact of head micromovements on functional connectomics. Neuroimage 76, 183–201.
Yan, C.G., Craddock, R.C., Zuo, X.N., Zang, Y.F., Milham, M.P., 2013b. Standardizing the intrinsic brain: towards robust measurement of inter-individual variation in 1000 functional connectomes. Neuroimage 80, 246–262.
Zhan, Y., Ma, J., Alexander-Bloch, A.F., Xu, K., Cui, Y., Feng, Q., Jiang, T., Liu, Y., Alzheimer's Disease Neuroimaging Initiative, 2016. Longitudinal study of impaired intra- and inter-network brain connectivity in subjects at high risk for Alzheimer's disease. J. Alzheimers Dis. 52, 913–927.
Zhao, Z., Lu, J., Jia, X., Chao, W., Han, Y., Jia, J., Li, K., 2014. Selective changes of resting-state brain oscillations in aMCI: an fMRI study using ALFF. Biomed. Res. Int. 2014, 920902.
Zou, Q., Miao, X., Liu, D., Wang, D.J., Zhuo, Y., Gao, J.H., 2015. Reliability comparison of spontaneous brain activities between BOLD and CBF contrasts in eyes-open and eyes-closed resting states. Neuroimage 121, 91–105.
Zuo, X.N., Di Martino, A., Kelly, C., Shehzad, Z.E., Gee, D.G., Klein, D.F., Castellanos, F.X., Biswal, B.B., Milham, M.P., 2010. The oscillating brain: complex and reliable. Neuroimage 49, 1432–1445.
Zuo, X.N., He, Y., Betzel, R.F., Colcombe, S., Sporns, O., Milham, M.P., 2017. Human connectomics across the life span. Trends Cogn. Sci. 21, 32–45.